Acoustic Tomography in Relation to 2D Ultrasonic Velocity and Hardness Mappings

Li Li, Xiping Wang, Lihai Wang and R. Bruce Allison

Abstract

Acoustic tomography is an emerging NDT technology for tree decay detection in both urban community and production forest. Many field studies have been conducted to assess the applicability and reliability of the technique in such applications. Although investigations on urban trees showed great success using acoustic tomography to detect moderate to severe internal decay within the trunk, detection of early stage of decay using such technology still constitutes a challenge This study was designed to evaluate the accuracy of acoustic tomography by analyzing the relationships between acoustic tomograms and two-dimensional mappings of ultrasonic properties and end hardness of the same trunk cross-sections. A freshly cut black cherry log was used to simulate a tree trunk and tested in the laboratory. Time-of-flight (TOF) acoustic tomography measurements were conducted at three different heights (10cm, 30cm, and 50 cm). A disc was then cut from each height and subjected to ultrasonic and mechanical evaluations. It was found that the acoustic shadows in the tomograms revealed internal structural defects that were at same locations and in similar magnitudes as the physical mappings of the discs. However, the shapes of the defect areas in the velocity and hardness mappings do not exactly match the acoustic shadows. Statistical analysis showed poor relationships between apparent velocity of the tomograms and measured ultrasonic velocity and end hardness. The acoustic tomograms obtained on the black cherry log represented a very narrow range of apparent velocity (COV=8.l-13.4%) in contrast to the wide range values for ultrasonic velocity (COV=33.8-37.3%) obtained from the discs. The results of this study suggest that TOF acoustic tomography has limited capability in detecting early stages of decay in trees.

Introduction

Internal decay is a major structural defect on trees of many species. The economic loss caused by internal decay is most significant for the hardwood trees that are used to produce appearance-grade veneer and other high value engineered wood products. Because of the exceptionally high prices paid for high quality hardwood trees, undetected decay can cause a substantial monetary loss to timber buyers and wood manufacturers (Wiedenbeck et al. 2004). Early detection of internal decay in hardwoods could provide a significant benefit to the industry in terms of making accurate quality assessments and volume estimates and use of the resource. It can also help foresters in prescribing silvicultural treatments for improved management decision-making and thus help maintain a healthy forest (Wang et al. 2009).

Acoustic tomography is an emerging NDT technology for tree decay detection in both urban community and production forest. It allows the users to visualize the velocity distribution of the

Li:
PhD Student, College of Engineering and Technology, Northeast Forestry University, Harbin, China
Wang:
Research Forest Products Technologist, USDA Forest Product Laboratory, Madison, WI, USA
Wang:
Professor, Dean, College of Engineering and Technology, Northeast Forestry University, Harbin, China
Allison:
Registered Consulting Arborist and Adjunct Professor of Dept. of Forest and Wildlife Ecology, University of Wisconsin, Madison, Madison, WI, USA

acoustic waves as the waves propagate through the cross section of a tree trunk. Because acoustic velocity is directly related to density and dynamic modulus of elasticity of wood, acoustic velocity mapping of a cross section could be used as a diagnostic image to detect internal decay in trees (Bucur 2003). The application of this technology was initially demonstrated on wooden poles by Tomikawa et al. (1990) for inspecting the internal condition of the poles. Later on, many researchers have investigated the applicability of the technology to detect internal decay in live trees (Comino et al. 2000; Gilbert and Smiley 2004; Wang et al. 2004, 2007, 2009; Allison et al. 2007; Deflorio 2008; Lin et al. 2008). So far, laboratory investigation and field application of acoustic tomography have been largely focused on urban trees with the principal goal being to determine the stability of the trees to minimize the risk of tree failure. The potential of this technology for assessing the quality of high-value hardwood trees in production forests has not been filly investigated. Although investigations on urban trees showed great success using acoustic tomography to detect moderate to severe internal decay within a trunk, the detection of early stage of decay using such technology still constitutes a challenge due to the facts that, 1) acoustic tomography techniques currently used are largely based on TOF measurements, which limit the accuracy and resolution of the tomography images obtained; 2) the construction of tomogram from TOF data is affected by pronounced anisotropy of tree species in terms of microstructures and wood properties; and 3) interpretation of tomograms is not quantitative in nature and often needs further confirmation or verification by other means.

The purpose of this experimental study was to quantitatively evaluate the accuracy of the TOF acoustic tomography for internal decay detection in trees and assess the capability of the technique for identifying decayed hardwood trees at an early stage of deterioration. The research approach was to examine the relationships between acoustic tomograms and two-dimensional mappings of ultrasonic velocity and end hardness of the same cross-section of a trunk.

Materials and Methods

A 1.2-m long freshly-cut black cherry (*Prunus serotina*) log containing heartwood decay was provided by the Wood Research Laboratory of the University of Wisconsin in Stevens Point for this study. The log was brought back to the USDA Forest Products Laboratory and put in a conditioning room (24°C and 66% relative humidity) immediately. To prevent the wood from drying, we covered the log with a plastic bag before starting acoustic tomography test.

Our laboratory experiment included three steps: 1) conduct acoustic tomography test at three heights (10 cm, 30 cm, and 50 cm) of the log section; 2) cut a 5-cm thick disc at each test height and conduct end hardness test on the cross section; and 3) cut each disc into 3cm by 3cm by 5 cm cubes and conduct ultrasonic transmission test on each small sample.

Acoustic Tomography Test

The black cherry log section was placed on the concrete floor vertically at the condition room to simulate a tree trunk in the field. A multi-channel acoustic measurement system, PiCUS® Sonic Tomograph (Argus Electronic Gmbh, Rostock, Germany), was used to conduct acoustic measurements on the "trunk" sample. The acoustic measurement system consisted of 12 sensors, which were evenly placed around the "trunk" in a horizontal plane. Each sensor was magnetically attached to a pin that was tapped into the bark and sapwood. TOFs of acoustic waves were measured by sequentially tapping each pin using the steel hammer. A complete TOF data matrix was obtained through this measurement process at each location. **Figure 1a** showed the experimental set up for TOF measurements on the black cherry "trunk" sample. **Figure 1b** showed the paths of TOF measurements for each tomography test.

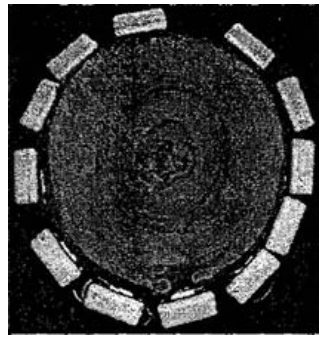

(a) Experimental set up

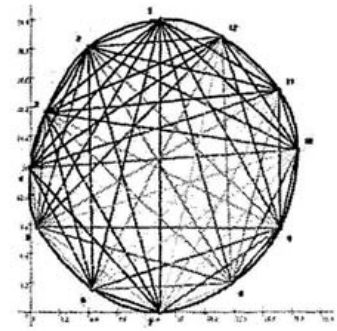

(b) Paths of TOF measurement

Figure 1.-*TOF acoustic tomography test.*

Acoustic TOF measurements were conducted at three different heights, 10cm, 30cm, and 50 cm above the "ground" (Laboratory floor). At each height, the circumference and distances between the sensors were measured using a tape measure and a PiCUS calliper. This information was used as an input for the system software to map the approximate geometric form of the cross-sections. Upon completion of the acoustic measurements, a two-dimensional (2D) velocity distribution (tomogram) was constructed for each cross-section using the PiCUS Q70 software (Argus Electronic Gmbh 2006).

After acoustic tomography test, a 5-cm thick disc was cut from each test height. The discs were then placed into plastic bags and kept in a controlled laboratory environment for further evaluation.

Hardness Test

In order to develop a hardness mapping of the cross section for each test height, we conducted end hardness on all three discs. The disc samples were first marked with 3 × 3 cm grids on the top surfaces. Hardness test was then conducted on each grid cell according to the Janka ball hardness test procedure given in ASTM D143-94 (ASTM 2005). The test setup (a standard 11.28 mm diameter steel ball mounted on the crosshead) allowed continuous recording of load as a function of the penetration depth of the steel ball into the wood. A threshold was set to automatically record the "maximum load" at an indentation of 5.64 mm as specified in ASTM D143-94. The experimental setup for hardness test is shown in **Figure 2.**

Ultrasonic Transmission Measurement

After completion of harness test, we cut each disc into 3 × 3 × 5 cm small samples along the grid lines. Each small sample was assigned with an *x-y* coordinate so that it can be traced back to its original position in the cross-section. A laboratory test bed was assembled to conduct ultrasonic transmission measurement on each small sample using a Sylvatest Duo device (CBT, St-Sulpice, Switzerland) **(Fig.3).**

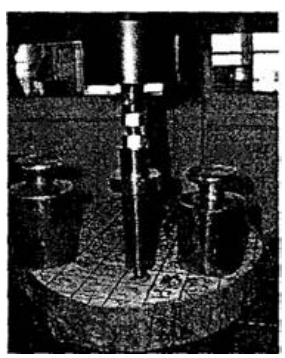

Figure 2.- *Hardness test on disc.*

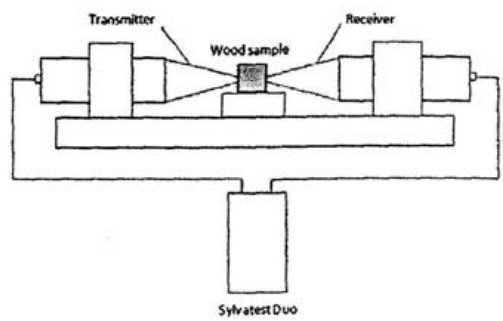

Figure 3.- *Ultrasonic transmission test on small samples.*

Two exponential piezoelectric conical transducers were used for transmitting and receiving the ultrasonic pulses. A constant pressure was applied to the sample and probes through a compressing air system. The ultrasonic transmission time was measured to an accuracy of ±1μs. For each small sample, ultrasonic transmission data was obtained at two orthogonal directions across the grain. In each direction, five ultrasonic transmission measurements were performed consecutively and an average transmission time value was displayed and recorded. Acoustic velocities were then calculated from recorded transmission time and the dimension of the samples.

Mapping of Ultrasonic Velocity and Hardness

Matlab software was used to construct maps of ultrasonic velocity and hardness for the three discs. Ultrasonic velocity and hardness data of each disc can be expressed in the following matrix form:

$$f(X,Y)=\begin{bmatrix} f(1,Y) & \cdots & f(X,Y) \\ \cdots & \cdots & \cdots \\ \cdots & \cdots & \cdots \\ f(1,1) & \cdots & f(X,1) \end{bmatrix} \quad [1]$$

The Matlab function adopted was contour f(X, Y, Z), where X and Y were coordinates of each grid cell, Z was measured ultrasonic velocity or hardness on each cell. This function was used to display isolines calculated from matrix Z and filled the areas between the isolines using constant colours corresponding to the figure's colour map. Another function adopted was interp2 (x, y, xi, yi, zi), which was used to improve the resolution of the mapping, and also gave the effect of "smoothing" out the data set.

Results and Discussion

The acoustic tomograms of the black cherry log section are shown in Figure 4 (*series i*). The acoustic tomogram showed distribution of apparent acoustic velocity in a cross-section of the log, where acoustic measurements were conducted. The colour presentation (brown (dark brown/light brown), green, and violet/blue/white) of acoustic shadows demonstrates the differences in the ability of the wood to transmit acoustic waves. Dark brown represents high acoustic velocity, high density, and sound wood; violet/blue/white represent areas of low velocity, low density, and unsound wood; and green represents the transition zone (barrier wall) between deteriorated and sound wood. The colour scale was expanded between the 100% and lowest velocity (Argus Electronic Gmbh 2006).

The acoustic tomograms indicated different levels of possible internal decay at three different heights (10 cm, 30 cm, and 50 cm). Acoustic shadows were the largest at the lower level (10 cm), and decreased progressively as the height increased. Physical examination of the discs at these locations confirmed the basic interpretation of the tomograms. It was found that the hollows, voids, and cracks on the discs are well reflected by the blue/white acoustic shadows in the tomograms.

The cross section mappings of measured ultrasonic velocity and end hardness of the black cherry discs are also shown in **Figure 4** (series ii and series iii). The colour scale of the maps is shown in the upper-right side of each map. The colour schemes used for the mappings are different from that for acoustic tomograms. But in general, dark blue represents very low velocity or hardness values, and dark red very high velocity or hardness values, with transition colours between the low and high velocity/hardness values. The blue colour on the periphery is the result of a mathematical treatment ("0" value) to form the boundary of the cross sections.

The mappings of measured ultrasonic velocity and end hardness show true physical conditions of the cross sections and therefore provide an objective standard for evaluating acoustic tomograms. Comparing with the acoustic tomograms, we found that the physical mappings of the log section revealed internal structural defects that are at same locations and in similar magnitudes as the acoustic shadows. However, the shapes of the defect areas in the velocity and hardness mappings do not exactly match the acoustic shadows in the tomograms. It should be pointed out that the resolution of velocity and hardness mappings is limited by the size of the small cubic samples (the smaller the sample size, the higher the resolution of the mappings). The smallest samples we can cut were determined by the ability of the testing equipment to properly conduct hardness and ultrasonic measurements.

Table 1 shows the statistics of the apparent acoustic velocity (tomograms) and measured ultrasonic velocity and end hardness (discs). Apparent velocity value at each cell on the cross section was extracted from the corresponding tomogram that was generated using a back projection algorithm (Gocke et al. 2007). The intersections of the "beelines" between the measurement points (sensor locations) determine an apparent acoustic velocity at each point **(Fig. 1b).**

Ultrasonic velocity of the small cubic samples was found significantly different at two orthogonal directions. This was primarily caused by grain orientation and local physical conditions. For example, in the case of sound sample, ultrasonic waves travelled faster in radial direction than that in tangential direction. In the case of defected sample (with both sound wood and defected wood), acoustic waves travelled faster through the path of solid wood than that through the path of defected wood (decay, voids, or checks). In **Table 1** and statistical analysis, we used lower value of measured velocity for each grid cell because we found that lower ultrasonic velocity had a better correlation with both the apparent acoustic velocity and end hardness.

Figure 5 (series i and ii) shows quantitative relationships between apparent acoustic velocity (tomograms) and measured ultrasonic velocity and end hardness. The best correlation was observed between apparent velocity and ultrasonic velocity for the disk at 30 cm, which had a correlation coefficient of $R^2 = 0.37$. In general, apparent velocity of the tomograms showed poor relationships with the measured ultrasonic velocity and end hardness. In comparing the velocity values, it was noted that apparent velocity of the tomograms had a very narrow range (COV= 8.1 - 13.4%), in contrast to the wide range values for ultrasonic velocity (COV=33.8 - 37.3%) obtained on the disks. This indicates that apparent velocity does not reflect the true velocity of the wood in a cross section, which is the inherent limitation of time-of-flight tomography. In tomography test, acoustic waves tend to avoid low-velocity zones. The resulting wave propagation path is often not the direct line between the sensors. Consequently, apparent velocities calculated based on direct distance of two sensors could be inflated, losing the sensitivity to low velocity features within a defected area.

From **Figure 5** (series iii), we observed a much better relationship between measured ultrasonic velocity and end hardness. However, the large variation of the relationship raised concerns on the accuracy of measurements on small cubic samples. In fact, both ultrasonic measurement and hardness measurement on the 3 × 3 cm samples were more or less affected by local defects and grain orientation. The ultrasonic velocity and end hardness measured might not be representative to the sample tested. This could have contributed to the poor relationships observed between apparent acoustic velocity and measured ultrasonic velocity and end hardness.

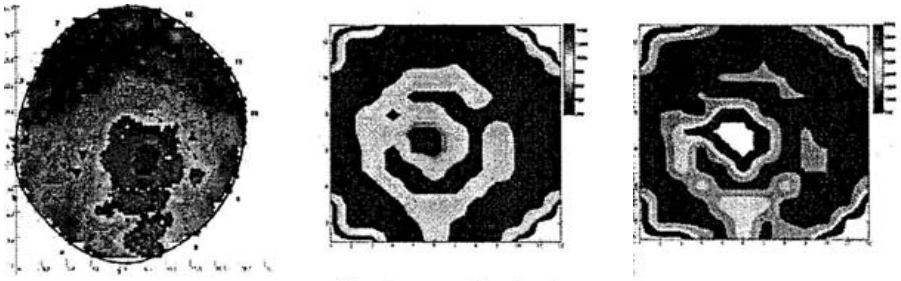

(i) Acoustic tomogram (ii) ultrasound velocity mapping (iii) Hardness mapping

a. Black cherry log-50 cm elevation

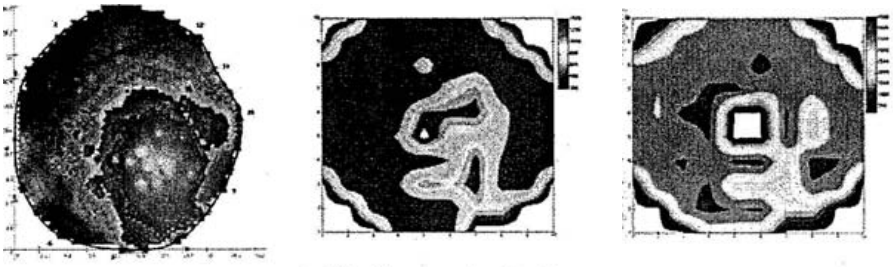

(i) Acoustic tomogram (ii) ultrasound velocity mapping (iii) Hardness mapping

b. Black cherry log-30 cm elevation

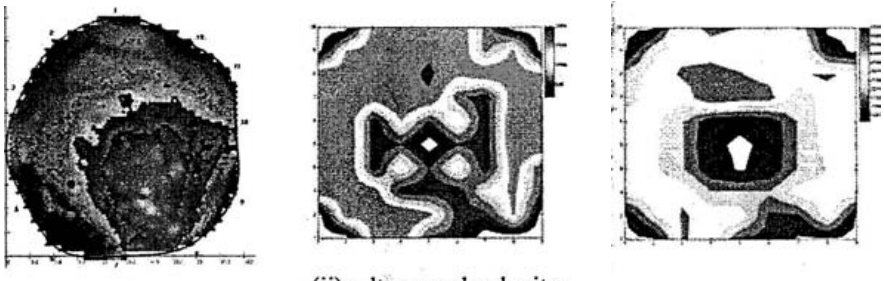

(i) Acoustic tomogram (ii) ultrasound velocity mapping (iii) Hardness mapping

c. Black cherry log-10 cm elevation

Figure 4.- *Acoustic tomograms, ultrasonic velocity mappings, and hardness mappings of the black cherry log section at 3 different heights.*

Table 1.- *Apparent acoustic velocity (tomogram) and measured ultrasonic velocity and end hardness of the black cherry log section.*

Log sample - Height	Apparent acoustic velocity (m/s)			Measured ultrasonic velocity (m/s)			End hardness (N)		
	Min.	Max.	COV (%)	Min.	Max.	COV (%)	Min.	Max.	COV (%)
50 cm	1072	1469	8.1	284	1815	37.3	19	5703	27.9
30 cm	898	1517	12.8	238	1858	36.8	14	5755	28.4
10 cm	1012	1659	13.4	298	1920	33.8	92	5551	32.6

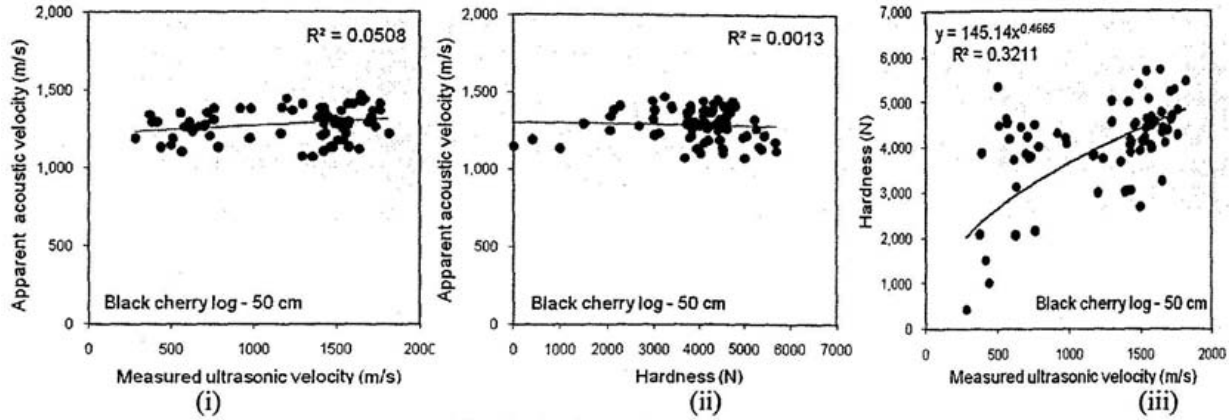

(a) Black cherry log - 50 cm.

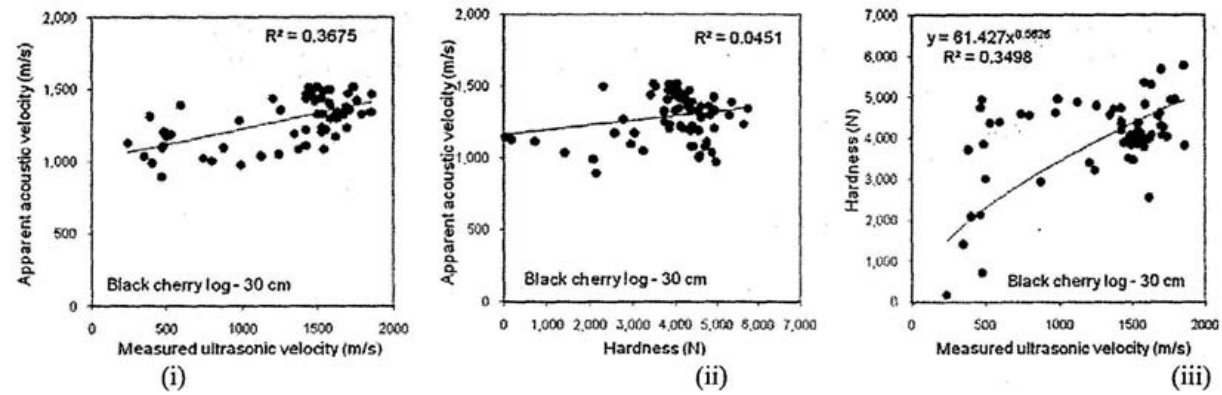

(b) Black cherry log - 30 cm

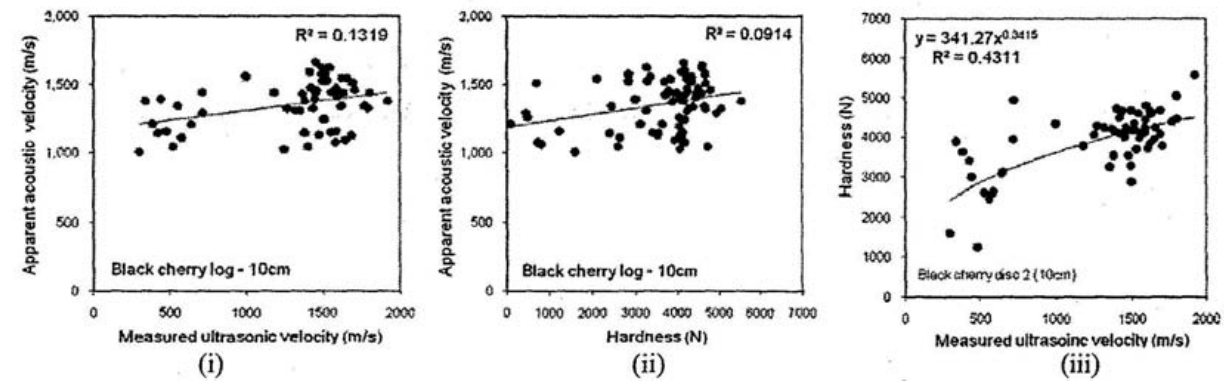

(c) Black cherry log - 10 cm

Figure 5.- *Quantitative relationships of (i) apparent acoustic velocity and measured ultrasonic velocity; (ii) apparent acoustic velocity and end hardness; and (iii) measured ultrasonic velocity and end hardness.*

Conclusions

This study was designed to evaluate the accuracy of TOF acoustic tomography by analyzing the relationships between acoustic tomograms and two-dimensional mappings of ultrasonic velocity and end hardness of the same cross-sections. Based on our laboratory experiments on a freshly cut black cherry log, we conclude the following:

The acoustic shadows in the tomograms revealed internal structural defects that were at same locations and in similar magnitudes as the physical mappings of the discs. However, the shapes of the defect areas in the velocity and hardness mappings do not exactly match the acoustic shadows.

Statistical analysis showed poor relationships between apparent acoustic velocity of the tomograms and measured ultrasonic velocity and end hardness.

Apparent velocity of the tomograms had a very narrow range (COV= 8.1 - 13.4%), in contrast to the wide range values for ultrasonic velocity (COV=33.8 - 37.3%) obtained on the disks. This indicates that apparent velocity does not reflect the true velocity of the wood in a cross section.

The results of this study suggest that TOF acoustic tomography has limited capability in detecting early stages of decay in trees.

Acknowledgment

This project was conducted under a cooperative research agreement between Northeast Forestry University, USDA Forest Products Laboratory, and University of Wisconsin Madison.

Literature Cited

Allison, R.B., Xiping Wang, and R.J. Ross. 2007. Visual and nondestructive evalution of red pines supporting a ropes course in the USFS Nesbit Lake Camp, Sidnaw, Michigan. In: Proceedings of the 15th International Symposium on Nondestructive Testing of Wood. Sept. 10-12, 2007, Duluth, MN, USA. Forest Products Society, Madison, Wisconsin. p. 43-48.

Argus Electronic Gmbh. 2006. PiCUS® Sonic Tomograph manual. Rostock, Germany.

ASTM. 2005. Standard methods of testing small clear specimens of timber. D 143-94. American Society for Testing and Materials, West Conshohocken, PA.

Bucur, V. 2003. Nondestructive characterization and imaging of wood. Springer-Verlag, Berlin, Heidelberg, Germany. 354 pp.

Comino, E., V. Socco, R. Martinis, G. Nicolotti and L. Sambuelli. 2000. Ultrasonic tomography for wood decay diagnosis. In: G.F. Backhaus, H. Balder and E. Idczak, Editors, International Symposium on Plant Health in Urban Horticulture, Braunschweig, Germany, 22–25May 2000, p. 279.

Deflorio, G., S. Fink, F.W.M. R. Schwarze. 2008. Detection of incipient decay in tree stems with sonic tomography after wounding and fungal inoculation. Wood Science and Technology 42: 117-132.

Gilbert, E.A and E.T. Smiley. 2004. PiCUS Sonic Tomograpgy for the quatification of decay in white oak (*Quercus Alba*) and hickory (*Carya spp.*). J Arboric 30(5): 277-280.

Gocke, L., S. Rust, U. Weihs, T. Gunther, and C. Rucker. 2008. Combining sonic and electrical impedance tomography for non-destructive testing of trees. In: Proceedings of the 15th International Symposium on Nondestructive Testing of Wood. Sept. 10-12, 2007, Duluth, MN, USA. Forest Products Society, Madison, Wisconsin. p. 3 1-42.

Lin, C., Y. Kao, T. Lin, M. Tsai, S. Wang, L. Lin, Y. Wang, M. Chan. 2008. Application of an ultrasonic tomographic technique for detecting defects in standing trees. International Biodeterioration & Biodegradation 62(2008): 434-441.

Tomikawa, Y.I., K. Arita and H. Yamada. 1990. Nondestructive inspection of wooden poles using ultrasonic computed tomography, IEEE Transactions UFFC 33 (4): 354–358.

Wang, X., F. Divos, C. Pilon, B.K. Brashaw, R.J. Ross, and R.F. Pellerin. 2004. Assessment of decay in standing timber using stress wave timing non-destructive evaluation tools - A guide for use and interpretation. Gen. Tech. Rep. FPL-GTR-147. Madison, WI: U.S. Department of Agriculture, Forest Service, Forest Products Laboratory. 12 pp.

Wang, X. and R.B. Allison. 2007. Decay detection in red oak trees using a combination of visual inspection, acoustic testing, and resistance microdrilling. J. Arboric Urban For 34(1): 1-4.

Wang, X., J. Wiedenbeck, S. Liang. 2009. Acoustic tomography for decay detection in black cherry trees. Wood and Fiber Science, 41(2): 127-137.

Wiedenbeck, J., M. Wiemann, D. Alderman, J. Baumgras, W. Luppold. 2004. Defining hardwood veneer log quality attribute. Gen. Tech. Rep. NE-313. USDA Forest Service, Northeastern Research Station. 36 pp.

Li, Li; Wang, Ziping; Wang, Lihai; Allison, Bruce 2009 Acoustic tomography in relation to 2D ultrasonic velocity and hardness mappings. In: Proceedings of the 16th nondestructive evaluation of wood symposium. 2009 October 12-14. Beijing, China. Beijing Forestry University: Beijing, China. Dr. Houjian Zhang and Dr. Xiping Wang, eds. p. 28-35.